

# Positioning the neutron drip line and the r-process paths in the nuclear landscape

Rui Wang<sup>1</sup> and Lie-Wen Chen<sup>\*1,2</sup>

<sup>1</sup>*Department of Physics and Astronomy and Shanghai Key Laboratory for Particle Physics and Cosmology, Shanghai Jiao Tong University, Shanghai 200240, China*

<sup>2</sup>*Center of Theoretical Nuclear Physics, National Laboratory of Heavy Ion Accelerator, Lanzhou 730000, China*  
(Dated: September 10, 2015)

Exploring nucleon drip lines and astrophysical rapid neutron capture process (r-process) paths in the nuclear landscape is extremely challenging in nuclear physics and astrophysics. While various models predict similar proton drip line, their predictions for neutron drip line and the r-process paths involving heavy neutron-rich nuclei exhibit a significant variation which hampers our accurate understanding of the r-process nucleosynthesis mechanism. Using microscopic density functional theory with a representative set of non-relativistic and relativistic interactions, we demonstrate for the first time that this variation is mainly due to the uncertainty of nuclear matter symmetry energy  $E_{\text{sym}}(\rho_{\text{sc}})$  at the subsaturation cross density  $\rho_{\text{sc}} = 0.11/0.16 \times \rho_0$  ( $\rho_0$  is saturation density), which reflects the symmetry energy of heavy nuclei. Using the recent accurate constraint on  $E_{\text{sym}}(\rho_{\text{sc}})$  from the binding energy difference of heavy isotope pairs, we obtain quite precise predictions for the location of the neutron drip line, the r-process paths and the number of bound nuclei in the nuclear landscape. Our results have important implications on extrapolating the properties of unknown neutron-rich rare isotopes from the data on known nuclei.

PACS numbers: 21.65.Ef, 21.10.Dr, 26.30.Hj, 21.60.Jz

**1. Introduction.**—The determination of the location of neutron and proton drip lines in the nuclear landscape is a fundamental question in nuclear physics. The drip lines tell us what is the limit of the nuclear stability against nucleon emission and how many bound nuclei can exist in the nuclear chart [1]. The quest for the neutron drip line (nDL) is also important for understanding the astrophysical rapid neutron capture process (r-process) which occurs along a path very close to the nDL in the nuclear landscape and provides a nucleosynthesis mechanism for the origin of more than half of the heavy nuclei in the Universe [2–5]. While the proton drip line (pDL) has been determined up to Protactinium (proton number  $Z = 91$ ) [6], there has little experimental information on the nDL for  $Z > 8$  [7]. Since the majority of rare isotopes inhabiting along the nDL and the r-process paths are unlikely to be observed in the terrestrial laboratory, their information has to rely on the model extrapolation based on the known nuclei, which is so far largely uncertain and hampers our accurate understanding of the r-process nucleosynthesis mechanism [8–11]. To understand and reduce the uncertainty of the model extrapolation from the known nuclei to the unknown neutron-rich rare isotopes is thus of critical importance, and we show here the symmetry energy plays a key role in this issue.

The nucleon drip lines are determined by nucleon separation energy of nuclei and theoretically they can be obtained from either macroscopic models [12–15] or microscopic density functional theory (DFT) [16–25]. Although these theoretical approaches have achieved remarkable success in describing the data on known nu-

clei, extrapolations to unknown nuclei appears less certain. Different approaches or interactions, which predict similar pDL, may give quite different predictions for the position of the nDL especially involving heavy neutron-rich nuclei [22–25]. Since the nuclei close to the nDL have extremely large isospin values, the model dependence is very likely related to the poorly known nuclear matter symmetry energy  $E_{\text{sym}}(\rho)$ , which characterizes the isospin dependent part of the equation of state (EOS) of asymmetric nuclear matter and is a key quantity to reflect the isovector properties of nuclear effective interactions (see, e.g., Ref. [26]). Indeed, Oyamatsu *et al.* [14] found a correlation between the nDL location and the density slope  $L(\rho_0)$  of the symmetry energy at saturation density  $\rho_0$ . However, a recent work by Afanasjev *et al.* [24] (see also Ref. [25]) provided no evidence for such a correlation, leaving a puzzle in the community. In this work, we demonstrate that the nDL location for heavy elements is actually correlated strongly by the magnitude of the symmetry energy at the subsaturation cross density (scaled by  $\rho_0$ )  $\rho_{\text{sc}} = 0.11/0.16 \times \rho_0$ , i.e.,  $E_{\text{sym}}(\rho_{\text{sc}})$ . In particular, the recent accurate constraint on  $E_{\text{sym}}(\rho_{\text{sc}})$  allows us to predict quite precisely the location of the nDL and thus the r-process paths as well as the number of bound nuclei in the nuclear landscape.

**2. The symmetry energy and drip lines.**—The symmetry energy plays multifaceted roles in nuclear physics and astrophysics [26–30] as well as new physics beyond the standard model [31], and it is defined as  $E_{\text{sym}}(\rho) = \frac{1}{2!} \frac{\partial^2 E(\rho, \delta)}{\partial \delta^2} |_{\delta=0}$  via an expansion of the nucleon specific energy (i.e., EOS) in an asymmetric nuclear matter, i.e.,  $E(\rho, \delta) = E_0(\rho) + E_{\text{sym}}(\rho)\delta^2 + O(\delta^4)$  where  $\rho$  is nucleon density and  $\delta = (\rho_n - \rho_p)/(\rho_p + \rho_n)$  is the isospin asymmetry. The  $E_0(\rho)$  represents the EOS of symmetric nuclear matter and is usually expanded around  $\rho_0$  as

---

\*Corresponding author (email: lwchen@sjtu.edu.cn)

$E_0(\rho) = E_0(\rho_0) + \frac{K_0}{2!}(\frac{\rho-\rho_0}{3\rho_0})^2 + O((\frac{\rho-\rho_0}{3\rho_0})^3)$  where the  $K_0$  is the so-called incompressibility coefficient. The symmetry energy  $E_{\text{sym}}(\rho)$  can be expanded around a reference density  $\rho_r$  as

$$E_{\text{sym}}(\rho) = E_{\text{sym}}(\rho_r) + L(\rho_r)\chi_r + O(\chi_r^2), \quad (1)$$

with  $\chi_r = \frac{\rho-\rho_r}{3\rho_r}$ . The coefficient  $L(\rho_r)$  denotes the density slope of the symmetry energy at  $\rho_r$ .

In the nuclear chart, all nuclei that can exist are bounded by the neutron and proton drip lines. Whether a nucleus can exist is determined by its single-nucleon and two-nucleon separation energy. Since the two-nucleon drip lines usually are more extended than the single-nucleon drip lines due to the pairing effect, in this work we thus mainly focus on the two-neutron (-proton) separation energy  $S_{2n}$  ( $S_{2p}$ ) of even-even nuclei and the corresponding two-neutron(-proton) drip line. The two-neutron (-proton) drip line location  $N_{\text{drip}}$  ( $Z_{\text{drip}}$ ) is recognized as the neutron (proton) number of the heaviest bound even-even nucleus within an isotope (isotone) chain which satisfy  $S_{2n} > 0$  ( $S_{2p} > 0$ ). It should be mentioned that there could exist a secondary and even a tertiary drip line for an isotope chain [22–25, 32] about which we do not consider in this work.

A qualitative preview about the two-nucleon drip lines can be obtained from the semi-empirical nuclear mass formula in which the binding energy of a nucleus with  $N$  neutrons and  $Z$  protons ( $A = N + Z$ ) is expressed as

$$B(N, Z) = a_{\text{vol}}A + a_{\text{surf}}A^{2/3} + a_{\text{sym}}(A)\frac{(N-Z)^2}{A} + a_{\text{coul}}\frac{Z(Z-1)}{A^{1/3}} + E_{\text{pair}}, \quad (2)$$

where  $a_{\text{vol}}$ ,  $a_{\text{surf}}$  and  $a_{\text{coul}}$  are constants,  $E_{\text{pair}}$  represents the pairing contribution, and  $a_{\text{sym}}(A)$  is the symmetry energy coefficient of finite nuclei. For a typical heavy nuclei around the nDL, such as  $^{222}\text{Er}$  ( $Z = 68$ ), assuming  $a_{\text{sym}}(A+2) \approx a_{\text{sym}}(A)$ , one can then obtain  $S_{2n} \approx -2a_{\text{vol}} - 0.22a_{\text{surf}} - 1.24a_{\text{sym}}(A) + 2.27a_{\text{coul}}$ . The pairing term is eliminated for even-even nuclei. Empirically, the values of  $a_{\text{vol}}$ ,  $a_{\text{surf}}$  and  $a_{\text{coul}}$  are relatively well determined, and thus the uncertainty of  $a_{\text{sym}}(A)$  (within a few MeV) essentially dominates the uncertainty of  $S_{2n}$  at large  $N - Z$  where the nDL is concerned and thus causes the uncertainty of the  $N_{\text{drip}}$ . Similarly, for a typical heavy nuclei around the pDL, such as  $^{222}\text{Cm}$  ( $Z = 96$ ), one has  $S_{2p} \approx -2a_{\text{vol}} - 0.22a_{\text{surf}} + 0.60a_{\text{sym}}(A) - 58.07a_{\text{coul}}$ . Since the pDL is close to the symmetry axis of  $N = Z$ , so  $a_{\text{sym}}(A)$  would not have a significant effect on  $S_{2p}$  and thus the pDL. In addition, the Coulomb energy makes  $S_{2p}$  vary very rapidly with  $Z$  and thus leads to a relatively stable  $Z_{\text{drip}}$ .

The above simple argument based on the mass formula thus indicates the  $a_{\text{sym}}(A)$  indeed plays a central role for locating the nDL. For heavy nuclei, considering the empirical correspondence between  $a_{\text{sym}}(A)$  and  $E_{\text{sym}}(\rho_c)$  [33–36] with  $\rho_c \approx 0.11 \text{ fm}^{-3}$  roughly corresponding to the nuclear average density, one then expects

$E_{\text{sym}}(\rho_{\text{sc}})$  (here  $\rho_c$  is replaced by  $\rho_{\text{sc}}$  to consider the saturation density variation in various models) should be strongly correlated with the  $N_{\text{drip}}$  for heavy elements.

**3. Correlation analysis.**—The present large-scale calculations of the nuclear binding energy are based on the Skyrme-Hartree-Fock-Bogolyubov (SHFB) approach using the code HFBTHO [37] and the relativistic mean field (RMF) approach using the code DIRBHZ [38]. These codes allow for an accurate description of deformation effects and pairing correlations in nuclei arbitrarily close to the nucleon drip lines. In particular, we use a large harmonic basis corresponding to 20 major shells and restrict ourselves to axially deformed nuclei. In the SHFB calculations, the density-dependent  $\delta$  pairing force with a mixed-type pairing is used and the pairing strength is adjusted to fit the empirical value of 1.245 MeV for the neutron pairing gap of  $^{120}\text{Sn}$  [18]. In DIRBHZ calculations, a separable version of finite range Gogny (D1S) pairing force is used [38]. In the following, we choose the Erbium isotope chain ( $Z = 68$ ) and isotone chain of  $N = 126$  as examples to evaluate  $N_{\text{drip}}$  and  $Z_{\text{drip}}$ , respectively, through which we hope to examine the correlation of the drip lines with different macroscopic quantities. The choice of isotope or isotone chain is more or less arbitrary, and the above choice is adopted to avoid the shell effect on the drip lines, about which we will discuss later.

For the standard Skyrme interaction (see, e.g., Ref. [39]), the nine parameters  $t_0$ - $t_3$ ,  $x_0$ - $x_3$  and  $\sigma$  can be expressed analytically in terms of nine macroscopic quantities  $\rho_0$ ,  $E_0(\rho_0)$ ,  $K_0$ ,  $E_{\text{sym}}(\rho_r)$ ,  $L(\rho_r)$ , the isoscalar effective mass  $m_{s,0}^*$ , the isovector effective mass  $m_{v,0}^*$ , the gradient coefficient  $G_S$  and the symmetry-gradient coefficient  $G_V$  [40]. In such a way, one can easily examine the correlations of nuclear structure properties with these macroscopic quantities by varying them individually within their empirical constraints [40]. By varying  $E_{\text{sym}}(\rho_{\text{sc}})$  while keeping other quantities, i.e.,  $\rho_0$ ,  $E_0(\rho_0)$ ,  $K_0$ ,  $L(\rho_{\text{sc}})$ ,  $m_{s,0}^*$ ,  $m_{v,0}^*$ ,  $G_S$ ,  $G_V$  and the spin-orbit coupling  $W_0$  at their default values in MSL1 [41], we show in Fig. 1 (a) by solid squares the  $N_{\text{drip}}$  for  $Z = 68$  as a function of  $E_{\text{sym}}(\rho_{\text{sc}})$ . As expected, it is seen that the  $N_{\text{drip}}$  exhibits a strong dependence on  $E_{\text{sym}}(\rho_{\text{sc}})$ , and it rapidly decreases with the increment of  $E_{\text{sym}}(\rho_{\text{sc}})$ . Similar analyses indicate that the  $N_{\text{drip}}$  is insensitive to  $L(\rho_{\text{sc}})$  and the  $Z_{\text{drip}}$  for  $N = 126$  displays very weak dependence on both  $E_{\text{sym}}(\rho_{\text{sc}})$  and  $L(\rho_{\text{sc}})$  as shown by the solid squares in Fig. 1 (b), (c) and (d), respectively. Applying the similar analysis to other macroscopic quantities, we find except that  $E_0$  and  $K_0$  show some effects on the  $N_{\text{drip}}$ , both the  $N_{\text{drip}}$  and  $Z_{\text{drip}}$  display essentially no dependence on all the other macroscopic quantities [42]. Since  $E_0$  and  $K_0$  are nowadays relatively well determined in the DFT, the  $E_{\text{sym}}(\rho_{\text{sc}})$  thus indeed plays a decisive role in locating the nDL.

In order to confirm the strong correlation between  $E_{\text{sym}}(\rho_{\text{sc}})$  and  $N_{\text{drip}}$  observed from the above simple correlation analyses, we also include in Fig. 1 the corresponding results with 42 other well-calibrated non-

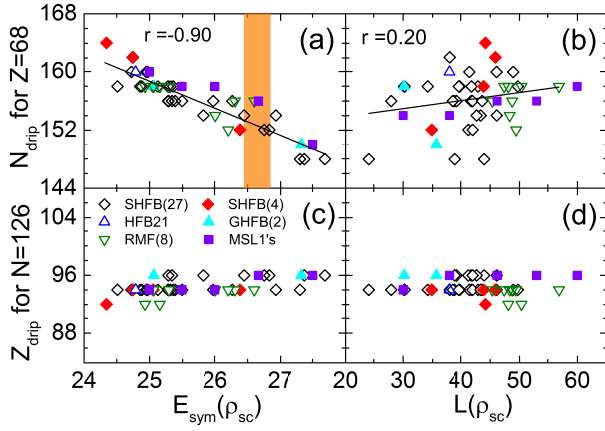


FIG. 1: (Color online) The calculated  $N_{\text{drip}}$  for  $Z = 68$  and  $Z_{\text{drip}}$  for  $N = 126$  versus  $E_{\text{sym}}(\rho_{\text{sc}})$  and  $L(\rho_{\text{sc}})$ . Solid squares are the results from SHFB calculations with MSL1 by varying individually  $E_{\text{sym}}(\rho_{\text{sc}})$  and  $L(\rho_{\text{sc}})$ . The results from other 42 non-relativistic and relativistic interaction are also included. The band in (a) indicates  $E_{\text{sym}}(\rho_{\text{sc}}) = 26.65 \pm 0.2$  MeV [41]. See text for details.

relativistic and relativistic interactions, namely, SHFB with 31 Skyrme interactions including 27 [43] (i.e., BSk14, SKM, RATP, SKT3, BSk11, BSk7, BSk10, SKT8, BSk5, SKT1, BSk4, BSk15, SKT6, MSK1, MSK2, BSk1, SKXce, SLy8, SLy4, SLy5, KDE, SLy9, Skz0,  $Z_{\sigma}^*$ , KDE0, Skz1 and a new Skyrme interaction MSL1\* [42]) obtained in this work and 4 (SV-min, UNEDF0, SKM\*, SkP) from Ref. [22], HFB with HFB21 [22, 44], Gogny-HFB (GHFB) with D1S and D1M [20, 21], and RMF model with 8 interactions including 5 [45, 46] (DD, DD-2, DD-ME1, TW99 and DD-F) obtained in this work and 3 (DD-PC1, DD-ME $\delta$ , DD-ME2) from Ref. [25]. We select these interactions in order to have a large spread of the  $E_{\text{sym}}(\rho_{\text{sc}})$  values within the empirical range of 24–28 MeV [35]. It is seen that the results from these interactions indeed follow the systematics from the simple correlation analysis above. The Pearson coefficient  $r$  for the  $N_{\text{drip}}-E_{\text{sym}}(\rho_{\text{sc}})$  correlation from the 43 interactions (including MSL1) is  $-0.90$ , and this is a pretty strong (anti-)correlation considering the fact that the  $N_{\text{drip}}$  is varied in unit of 2. In addition, one can also see from Fig. 1 that the  $N_{\text{drip}}$  from the 43 interactions exhibits a very weak correlation with the  $L(\rho_{\text{sc}})$  ( $r = 0.20$ ), and both  $E_{\text{sym}}(\rho_{\text{sc}})$  and  $L(\rho_{\text{sc}})$  essentially have no effects on the  $Z_{\text{drip}}$ .

It is interesting to examine the correlations of the  $N_{\text{drip}}$  for  $Z = 68$  with  $E_{\text{sym}}(\rho_0)$  and  $L(\rho_0)$ , and the results are plotted in Fig. 2 using the 43 interactions. It is seen that both the correlations are quite weak, i.e., the  $r$  value is  $-0.32$  for  $N_{\text{drip}}-E_{\text{sym}}(\rho_0)$  and  $0.28$  for  $N_{\text{drip}}-L(\rho_0)$ , consistent with the conclusion in Refs. [24, 25]. This feature is due to the fact that the  $N_{\text{drip}}$  depends on both  $E_{\text{sym}}(\rho_0)$  and  $L(\rho_0)$  due to their correlation with  $E_{\text{sym}}(\rho_{\text{sc}})$  [34]. Furthermore, if  $E_{\text{sym}}(\rho_0)$  ( $L(\rho_0)$ ) is fixed, increasing  $L(\rho_0)$  (decreasing  $E_{\text{sym}}(\rho_0)$ ) will lead to a de-

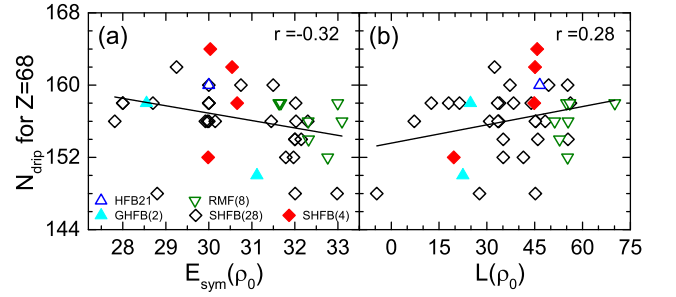


FIG. 2: (Color online) The calculated  $N_{\text{drip}}$  for  $Z = 68$  versus  $E_{\text{sym}}(\rho_0)$  and  $L(\rho_0)$  from 43 non-relativistic and relativistic interactions. See text for details.

crease of  $E_{\text{sym}}(\rho_{\text{sc}})$  [34] and thus an increase of  $N_{\text{drip}}$ , consistent with the results in Ref. [14].

**4. Neutron drip line and  $r$ -process path.**—The above analyses suggest a precise value of  $E_{\text{sym}}(\rho_{\text{sc}})$  will put stringent constraint on the location of the nDL and the  $r$ -process paths. Using the accurate constraint of  $E_{\text{sym}}(\rho_{\text{sc}}) = 26.65 \pm 0.2$  MeV extracted recently by analyzing the binding energy difference of heavy isotope pairs [41], one can thus obtain the drip lines by using five of the previous 43 interactions, i.e., KDE, SLy4, MSL1, MSL1\* and DD-ME1, which are consistent with  $E_{\text{sym}}(\rho_{\text{sc}}) = 26.65 \pm 0.2$  MeV (see the band in Fig. 1 (a)), and the results are shown in Fig. 3. Also included in Fig. 3 are the experimentally known even-even nuclei. The recently measured light neutron-unbound nuclei  $^{16}\text{Be}$  [48] and  $^{26}\text{O}$  [49] are not included. It is very interesting to see that these interactions indeed give quite similar predictions for both the neutron and proton drip lines. In light mass region where the DFT calculation is expected to be less reliable, while KDE, SLy4, MSL1 and DD-ME1 predict  $^{26}\text{O}$  or  $^{28}\text{O}$  to be the two-neutron drip line of Oxygen, MSL1\* predicts  $^{24}\text{O}$  which agrees with the current experimental suggestion [49]. In addition, we note that a small variation of other parameters can easily vary  $N_{\text{drip}}$  by 2 for Oxygen [42]. It should be mentioned that the lighter two-neutron drip line nucleus  $^{24}\text{O}$  can also be predicted by considering the repulsive three-body force [50].

Also included in Fig. 3 are the drip lines from the Weizsacker-Skyrme mass formula with the most recent parameter set WS4 [15] which predicts a quite small rms deviation of 298 keV with respect to essentially all the available mass data, and they are seen to agree well with the five microscopic calculations. We would like to point out that all the five microscopic predictions are consistent with the benchmark calculations [22–25] (the gray band in Fig. 3) but with a much smaller uncertainty, indicating the importance of an accurate value of  $E_{\text{sym}}(\rho_{\text{sc}})$ .

The precise position of the two-nucleon drip lines allows us to estimate the number of bound even-even nuclei with  $2 \leq Z \leq 120$ , and the result is 1887 for KDE, 1928 for SLy4, 1975 for MSL1, 1953 for MSL1\* and 1963 for DD-ME1, indicating a quite precise value of

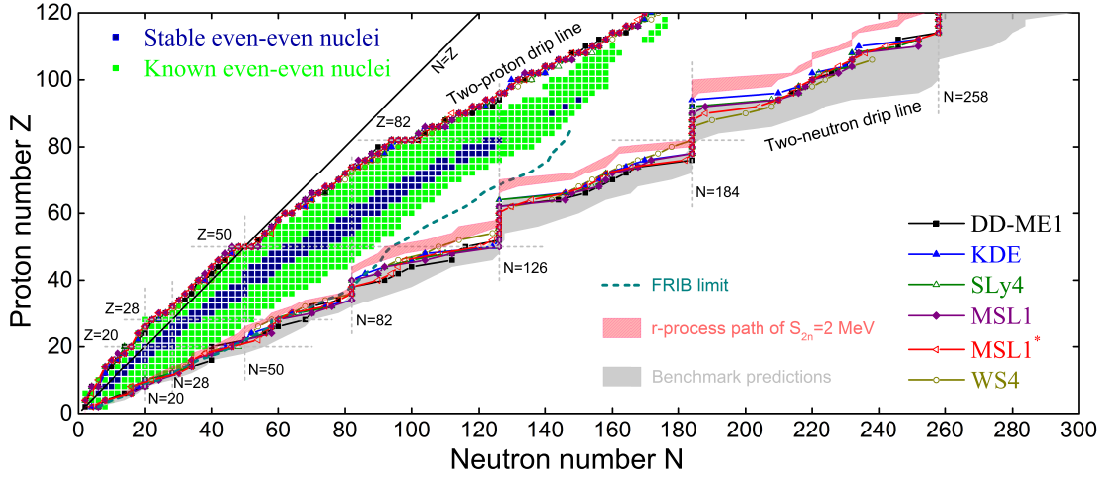


FIG. 3: (Color online) The landscape of bound even-even nuclei as obtained from DFT calculations with four Skyrme interactions (KDE, SLy4, MSL1, MSL1\*) and one relativistic interaction (DD-ME1). The prediction from Weizsacker-Skyrme mass formula with WS4 [15] is also included for comparison. The gray band denotes the uncertainty of two-neutron drip line from the benchmark calculations in Refs. [22–25]. The red band shows the r-process path of  $S_{2n} = 2$  MeV for KDE, SLy4, MSL1, MSL1\* and DD-ME1. The experimentally known 800 bound even-even nuclei (up to 2014), including 169 stable (navy squares) and 631 radioactive (green squares), are extracted from Ref. [47] and references therein.

$1941 \pm 31$  (only 800 have been discovered experimentally [47]). The uncertainty mainly comes from the shell effect which will be discussed later. Furthermore, the single-nucleon drip lines can be estimated from the condition  $-E_{n,p}^F(N, Z) = \Delta_{n,p}(N, Z)$  while the two-n(p)DL of odd- $Z(N)$  nuclei can be estimated from the condition  $2E_{n(p)}^F(N, Z) = 0$ , where the Fermi energy  $E^F$  and pairing gap  $\Delta$  of odd-odd or odd- $A$  nuclei can be approximated by the average of the corresponding calculated results of their even-even neighbors [22]. Accordingly, we estimate the total number of bound nuclei to be 6794, 6895, 7115 and 6659 for KDE, SLy4, MSL1 and MSL1\*, respectively, leading to a precise estimate of  $6866 \pm 166$  (only 3191 have been discovered experimentally [47]). Although the above candidate interactions are not a large sample, the small variation of their predictions represents a useful estimate of the uncertainty from sources other than  $E_{\text{sym}}(\rho_{\text{sc}})$ .

The astrophysical r-process is expected to occur along a path of constant neutron separation energies [2–5, 8–11]. For the five candidate interactions, we also include in Fig. 3 the r-process path of  $S_{2n} = 2$  MeV (the results with other  $S_{2n}$  values can be provided by the authors on request). One can see the five interactions give fairly consistent r-process paths. Further shown in Fig. 3 is the limit of neutron-rich isotopes that might be measured at FRIB [51, 52], and our results suggest that the future FRIB experiment measurement may cover the nDL for  $Z \lesssim 30$  and  $Z \approx 40$  as well as the r-process path for  $Z \lesssim 50$  and  $Z \approx 70$ .

As shown in Fig. 3, the nDL exhibits a clear shell structure, i.e., around neutron magic numbers  $N = 82, 126, 184$  and  $258$ , the position of the nDL is robust. However, the  $Z$  value ( $Z_{\text{sh}}$ ) at which the nDL moves away

from the neutron magic number is sensitive to the interactions, and this is the main reason for the small variation in the predicted number of bound nuclei from the candidate interactions as mentioned earlier. Using a similar analysis as before, we find that the  $Z_{\text{sh}}$  value is sensitive to all macroscopic quantities, i.e.,  $\rho_0$ ,  $E_0(\rho_0)$ ,  $K_0$ ,  $m_{s,0}^*$ ,  $m_{v,0}^*$ ,  $G_S$ ,  $G_V$ ,  $W_0$ ,  $E_{\text{sym}}(\rho_{\text{sc}})$  and  $L(\rho_{\text{sc}})$  [42], indicating the complexity of an accurate prediction of the  $Z_{\text{sh}}$  value.

**5. Conclusion.**—In summary, using microscopic density functional theory with a number of representative non-relativistic and relativistic interactions, we have found a strong correlation between the neutron drip line location and the magnitude of the symmetry energy  $E_{\text{sym}}(\rho_{\text{sc}})$  at the subsaturation cross density (scaled by  $\rho_0$ )  $\rho_{\text{sc}} = 0.11/0.16 \times \rho_0$ . This finding together with the recent accurate constraint on  $E_{\text{sym}}(\rho_{\text{sc}})$  from the binding energy difference of heavy isotope pairs allows us to obtain quite precise predictions for the location of the neutron drip line, the r-process paths and the number of bound nuclei in the nuclear landscape. Our work sheds light on extrapolating the properties of unknown neutron-rich rare isotopes from the data on known nuclei. The present results should be less model dependent since they are based on a large set of both non-relativistic and relativistic models. In addition, although we have only used the lowest-order (quadratic) symmetry energy term  $E_{\text{sym}}(\rho)$  to characterize the isospin-dependent part of the EOS for asymmetric nuclear matter, all the higher-order symmetry energy terms have been considered self-consistently in the mean-field calculations.

**Acknowledgments.**—We thank S. Goriely for providing us the data of Gogny-HFB calculations, N. Wang for WS4 data, and Z. Zhang for the help with constructing the MSL1\* interaction. We would also like to thank C.



M. Ko, B. A. Li, and W. Nazarewicz for very helpful discussions and comments. This work was supported in part by the National Basic Research Program of China (973 Program) under Contracts No. 2013CB834405 and No. 2015CB856904, the NNSF of China under Grant Nos. 11275125 and 11135011, the “Shu Guang” project

supported by Shanghai Municipal Education Commission and Shanghai Education Development Foundation, the Program for Professor of Special Appointment (Eastern Scholar) at Shanghai Institutions of Higher Learning, and the Science and Technology Commission of Shanghai Municipality (11DZ2260700).

- 
- [1] M. Thoennessen, Rep. Prog. Phys. **67**, 1187 (2004).
  - [2] J.J. Cowan, F.-K. Thielemann, and J.W. Truran, Phys. Rep. **208**, 267 (1991).
  - [3] K. Langanke and M. Wiescher, Rep. Prog. Phys. **64**, 1657 (2001).
  - [4] Y.-Z. Qian, Prog. Part. Nucl. Phys. **50**, 153 (2003).
  - [5] M. Arnould, S. Goriely, and K. Takahashi, Phys. Rep. **450**, 97 (2007).
  - [6] National Nuclear Data Centre. Evaluated Nuclear Structure Data File. <http://www.nndc.bnl.gov/ensdf/>.
  - [7] T. Baumann *et al.*, Nature **449**, 1022 (2007).
  - [8] S. Goriely and M. Arnould, Astron. Astrophys. **262**, 73 (1992); S. Wanajo, S. Goriely, M. Samyn, and N. Itoh, Astrophys. J. **606**, 1057 (2004).
  - [9] K.-L. Kratz, J.-P. Bitouzet, F.-K. Thielemann, P. Moller, and B. Pfeiffer, Astrophys. J. **403**, 216 (1993); K.-L. Kratz, K. Farouqi, and P. Moller, Astrophys. J. **792**, 6 (2014).
  - [10] B. Sun *et al.*, Phys. Rev. C **78**, 025806 (2008).
  - [11] J. Van Schelt *et al.*, Phys. Rev. Lett. **111**, 061102 (2013).
  - [12] P. Möller, J.R. Nix, W.D. Myers, and W.J. Swiatecki, At. Data Nucl. Data Tables **59**, 185 (1995).
  - [13] J. Duflo and A.P. Zuker, Phys. Rev. C **52**, R23 (1995).
  - [14] K. Oyamatsu, K. Iida, and H. Koura, Phys. Rev. C **82**, 027301 (2010).
  - [15] N. Wang, M. Liu, X.Z. Wu, and J. Meng, Phys. Lett. **B734**, 215 (2014).
  - [16] J. Dobaczewski, H. Flocard, and J. Treiner, Nucl. Phys. **A422**, 103 (1984); M.V. Stoitsov, J. Dobaczewski, W. Nazarewicz, S. Pittel, and D.J. Dean, Phys. Rev. C **68**, 054312 (2003); M.V. Stoitsov, W. Nazarewicz, and N. Schunck, Int. J. Mod. Phys. E **18**, 816 (2009).
  - [17] D. Hirata *et al.*, Nucl. Phys. **A616**, 438c (1997).
  - [18] J. Dobaczewski, W. Nazarewicz, and M.V. Stoitsov, Eur. Phys. J. A **15**, 21 (2002).
  - [19] L. Geng, H. Toki, and J. Meng, Prog. Theor. Phys. **113**, 785 (2005).
  - [20] S. Goriely, S. Hilaire, M. Girod, and S. Péru, Phys. Rev. Lett. **102**, 242501 (2009).
  - [21] J.-P. Delaroche *et al.*, Phys. Rev. C **81**, 014303 (2010).
  - [22] J. Erler *et al.*, Nature **486**, 509 (2012).
  - [23] J. Erler, C.J. Horowitz, W. Nazarewicz, M. Rafalski, and P.-G. Reinhard, Phys. Rev. C **87**, 044320 (2013).
  - [24] A.V. Afanasjev, S.E. Agbemava, D. Ray, and P. Ring, Phys. Lett. **B726**, 680 (2013).
  - [25] S.E. Agbemava, A.V. Afanasjev, D. Ray, and P. Ring, Phys. Rev. C **89**, 054320 (2014).
  - [26] B.A. Li, L.W. Chen, and C.M. Ko, Phys. Rep. **464**, 113 (2008).
  - [27] B.M. Tsang *et al.*, Phys. Rev. C **86**, 015803 (2012).
  - [28] J.M. Lattimer, Ann. Rev. Nucl. Part. Sci. **62**, 485 (2012).
  - [29] P. Donati, P.M. Pizzochero, P.F. Bortignon, and R.A. Broglia, Phys. Rev. Lett. **72**, 2835 (1994).
  - [30] D.J. Dean, K. Langanke, and J.M. Sampaio, Phys. Rev. C **66**, 045802 (2002).
  - [31] C.J. Horowitz, S.J. Pollock, P.A. Souder, and R. Michaels, Phys. Rev. C **63**, 025501 (2001); T. Sil, M. Centelles, X. Viñas, and J. Piekarewicz, Phys. Rev. C **71**, 045502 (2005); P.G. Krastev and B.A. Li, Phys. Rev. C **76**, 055804 (2007); D.H. Wen, B.A. Li, and L.W. Chen, Phys. Rev. Lett. **103**, 211102 (2009); H. Zhang, Z. Zhang, and L.W. Chen, JCAP **08**, 011 (2014).
  - [32] Y.N. Zhang, J.C. Pei, and F.R. Xu, Phys. Rev. C **88**, 054305 (2013).
  - [33] M. Centelles, X. Roca-Maza, X. Viñas, and M. Warda, Phys. Rev. Lett. **102**, 122502 (2009).
  - [34] L.W. Chen, Phys. Rev. C **83**, 044308 (2011).
  - [35] P. Danielewicz and J. Lee, Nucl. Phys. **A922**, 1 (2014).
  - [36] F.J. Fattoyev, W.G. Newton, and B.A. Li, Phys. Rev. C **90**, 022801(R) (2014).
  - [37] M.V. Stoitsov, J. Dobaczewski, W. Nazarewicz, and P. Ring, Comp. Phys. Comm. **167**, 43 (2005).
  - [38] T. Nikšić, N. Paar, D. Vretenar, and P. Ring, Comp. Phys. Comm. **185**, 1808 (2014).
  - [39] E. Chahanat, P. Bonche, P. Haensel, J. Meyer, and R. Schaeffer, Nucl. Phys. **A627**, 710 (1997); Nucl. Phys. **A635**, 231 (1998); erratum **643**, 441 (1998).
  - [40] L.W. Chen, C.M. Ko, B.A. Li, and J. Xu, Phys. Rev. C **82**, 024321 (2010); L.W. Chen and J.Z. Gu, J. Phys. G **39**, 035104 (2012).
  - [41] Z. Zhang and L.W. Chen, Phys. Lett. **B726**, 234 (2013).
  - [42] R. Wang, Z. Zhang, and L.W. Chen, in preparation, 2015.
  - [43] R. Chen *et al.*, Phys. Rev. C **85**, 024305 (2012).
  - [44] S. Goriely, N. Chamel, and J.M. Pearson, Phys. Rev. C **82**, 035804 (2010).
  - [45] L.W. Chen, C.M. Ko, and B.A. Li, Phys. Rev. C **76**, 054316 (2007).
  - [46] S. Typel, G. Ropke, T. Klahn, D. Blaschke, and H.H. Wolter, Phys. Rev. C **81**, 015803 (2010).
  - [47] M. Thoennessen, Rep. Prog. Phys. **76**, 056301 (2013); Int. J. Mod. Phys. E **23**, 1430002 (2014); Int. J. Mod. Phys. E **24**, 1530002 (2015).
  - [48] A. Spyrou *et al.*, Phys. Rev. Lett. **108**, 102501 (2012).
  - [49] E. Lunderberg *et al.*, Phys. Rev. Lett. **108**, 142503 (2012).
  - [50] T. Otsuka *et al.*, Phys. Rev. Lett. **105**, 032501 (2010).
  - [51] A.V. Afanasjev *et al.*, Phys. Rev. C **91**, 014324 (2015).
  - [52] FRIB Estimated Rates, Version 1.06, <http://groups.nsl.msui.edu/frib/rates/fribrates.html>.